

The CHAOS-3 Geomagnetic Field Model and Candidates for IGRF-2010

Nils Olsen^{1*}; Mioara Mandea^{2†}; Terence J. Sabaka³, Lars Tøffner-Clausen¹

¹DTU Space, Juliane Maries Vej 30, 2100 Copenhagen, Denmark

²Université Paris Diderot, IPG Paris, Géophysique spatiale et planétaire,
Bâtiment Lamarck, 5 rue Thomas Mann, 75013 Paris, France

³Geodynamics Branch, NASA GSFC, Greenbelt/MD, USA

Draft, October 2, 2009

1 Introduction

The parent model for our IGRF candidates is CHAOS-3, which is an update of the CHAOS-2 model of *Olsen et al.* [2009].

Main differences are:

- CHAMP and Ørsted data are taken up to August 2009 (CHAOS-2: March 2009)
- Revised observatory monthly means (using the approach developed by *Olsen* [2009]) are taken for the time January 1997 to January 2009.
- The third time derivative of the squared magnetic field intensity is regularized at the Core-Mantle-Boundary (CMB).

2 Data

We use Ørsted scalar and vector data between March 1999 and July 2009 (vector data only until December 2005), CHAMP vector and scalar data between August 2000 and August 2009 (vector data only after January 2001), and SAC-C scalar data between January 2001 and December 2004. Same data selection criteria as for CHAOS-2 have been applied.

*also at Niels Bohr Institute of Copenhagen University, Juliane Maries Vej 30, 2100 Copenhagen, Denmark

†formerly at Helmholtz-Zentrum Potsdam, Deutsches GeoForschungsZentrum, D-14473 Potsdam, Germany

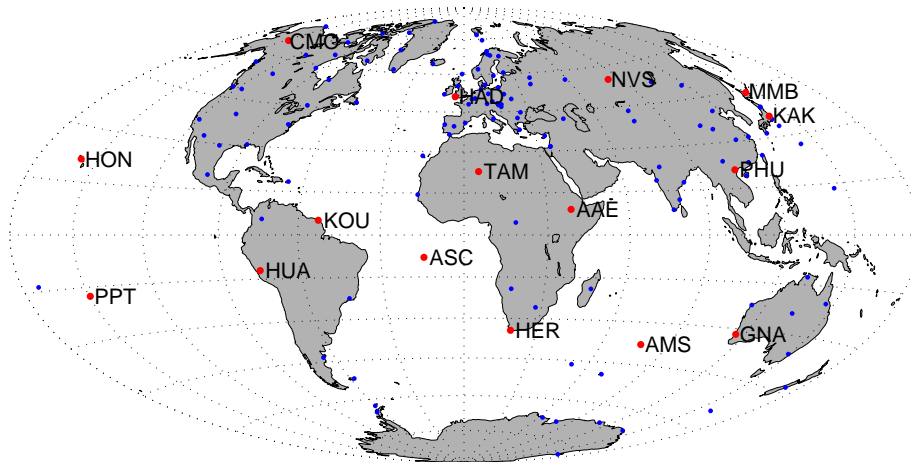


Figure 1: Location of the 137 observatories used for CHAOS-3 (blue symbols). Emphasized (with red symbols) are the 16 observatories which data are shown in Figs. 5 and 6

To extend the model back in time beyond February 1999 we augment with annual differences of revised observatory monthly means of the North, East and downward components (X, Y, Z) for the years 1997 to 2008. However, as opposed to CHAOS-2, for which we used monthly means calculated in the traditional way as the arithmetic mean of all data of a given month, for CHAOS-3 we use *revised* monthly mean values. These are calculated in the following way: From the observatory hourly mean values we remove a model of the ionospheric (plus induced) field as predicted by the CM4 model [Sabaka *et al.*, 2004], parameterized by 3-monthly means of $F_{10.7}$ solar flux, and of the magnetospheric (plus induced) contributions as predicted by the external field part of CHAOS-2, parameterized by the E_{st} and I_{st} indices. We then calculate the robust mean value (using Huber weights with tuning constant of 1.5) from all hourly mean values of a given month, each observatory, and each of the three elements X, Y and Z . Finally we take annual differences of the revised monthly means (annual difference means that the value at time t is obtained by taking the difference between those at $t + 6$ months and $t - 6$ months, thereby eliminating an annual variation in the data). This yields 15,756 values of the first time derivative of the vector components, $(dX/dt, dY/dt, dZ/dt)$ for 137 observatories. The location of these observatories are shown in Figure 1.

3 Model parameterization and Regularization

The time dependence of core field coefficients up to spherical harmonic degree $n = 20$ is described by order 6 B-splines with a 6-month knot separation and five-fold knots at the endpoints, $t = 1997.0$ and $t = 2010.0$. This yields 27 inte-

rior knots (at 1997.5, 1998.0, . . . , 2009.5) and 6 exterior knots at each endpoint, 1997.0 and 2010.0, resulting in 31 basic B-spline functions, $M_i(t)$. Internal field coefficients for degrees $n = 21 - 60$ are static. Time-dependent terms (for degrees $n = 1 - 20$) and static terms (for $n = 21 - 60$) together results in a total of 16,920 internal Gauss coefficients.

Large-scale external (magnetospheric) sources are parameterized similar as for the CHAOS-2 model, with an expansion of far magnetospheric sources (magnetotail and magnetopause) in *Geocentric Solar Magnetospheric (GSM)* coordinates (up to $n = 2$) and of near magnetospheric sources (magnetospheric ring current) in the *Solar Magnetic (SM)* coordinate system (also up to $n = 2$). The time dependence of degree-1 magnetospheric terms in SM coordinates is parameterized by the E_{st} and I_{st} indices [Maus and Weidelt, 2004; Olsen et al., 2005]. In addition, we solve for large-scale time-varying degree-1 coefficients in bins of 12 hours length (for $n = 1, m = 0$), resp. 5 days length (for $n = m = 1$), similar as for the CHAOS-2 model. This gives a total of 6,151 external coefficients.

Finally, we perform an in-flight instrument calibration and solve for the Euler angles of the rotation between the coordinate systems of the vector magnetometer and of the star sensor that provide attitude information. For the Ørsted data, this yields two sets of Euler angles, while for CHAMP we solve for Euler angles in bins of 10 days (i.e. 204 sets of angles). This yields additional $3 \times (2 + 204) = 618$ model parameters. The total number of model parameters is $16,920 + 6,151 + 618 = 23,689$.

These model parameters are estimated by means of a regularized *Iteratively Reweighted Least-Squares* approach using Huber weights, minimizing the cost function

$$\mathbf{e}^T \underline{\underline{C}}^{-1} \mathbf{e} + \lambda_3 \mathbf{m}^T \underline{\underline{\Lambda}}_3 \mathbf{m} + \lambda_2 \mathbf{m}^T \underline{\underline{\Lambda}}_2 \mathbf{m} \quad (1)$$

where \mathbf{m} is the model vector, the residuals vector $\mathbf{e} = \mathbf{d}_{obs} - \mathbf{d}_{mod}$ is the difference between observation \mathbf{d}_{obs} and model prediction \mathbf{d}_{mod} , and $\underline{\underline{C}}$ is the data covariance matrix.

$\underline{\underline{\Lambda}}_3$ and $\underline{\underline{\Lambda}}_2$ are block diagonal regularization matrices which constrains the third, resp. second order time derivatives of the core field. $\underline{\underline{\Lambda}}_3$ minimizes the mean squared magnitude of $\left| \frac{\partial^3 \mathbf{B}}{\partial t^3} \right|$, integrated over the core surface $d\Omega$ (radius $c = 3485$ km) and averaged over time:

$$\left\langle \left| \frac{\partial^3 \mathbf{B}}{\partial t^3} \right|^2 \right\rangle = \frac{1}{\Delta t} \int_{t=1997}^{2010} \int \left| \frac{\partial^3 \mathbf{B}}{\partial t^3} \right|^2 d\Omega dt = \mathbf{m}^T \underline{\underline{\Lambda}}_3 \mathbf{m}. \quad (2)$$

We found that regularization of the third time derivative alone leads to highly oscillating field behavior. To avoid this we also minimize $|\ddot{\mathbf{B}}|^2$ at the CMB at the model endpoints $t = 1007.0$ and 2010.0 . This is implemented via the regularization matrix $\underline{\underline{\Lambda}}_2$. Note that $\underline{\underline{\Lambda}}_2$ only acts on the first and last 6 (out of 31) spline basis functions.

This regularization is different from that used for CHAOS-2 (for which the time average of the second time derivative, $|\ddot{\mathbf{B}}|^2$, is minimized at the core surface). However, we also derived a model using the same model parameterization

Table 1: Number N of data points, mean, and rms misfit (in nT for the satellite data, and in nT/yr for the observatory data) for CHAOS-3.

		component	N	CHAOS-3	
				mean	rms
satellite	all	F_{polar}	298771	-0.03	5.50
		$F_{\text{nonpolar}} + B_B$	824864	0.04	2.40
	Ørsted	F_{polar}	114312	0.89	4.29
		$F_{\text{nonpolar}} + B_B$	412765	0.42	2.27
		B_{\perp}	144515	-0.00	7.73
	CHAMP	B_3	144515	-0.04	3.63
		F_{polar}	149130	-0.87	6.65
		$F_{\text{nonpolar}} + B_B$	268559	-0.59	2.50
		B_{\perp}	254289	0.01	4.58
	SAC-C	B_3	254289	0.09	3.21
		F_{polar}	35329	0.02	4.22
		F_{nonpolar}	143540	0.13	2.57
observatory		dX/dt	15,756	0.02	7.35
		dY/dt	15,756	-0.02	5.02
		dZ/dt	15,756	-0.10	7.02

(and regularization) as CHAOS-2s but the updated data set of CHAOS-3; we will in following refer to this as the “updated CHAOS-2s” model.

4 Results and Discussion

Number of data points, residual means and root mean squared (rms) values of the two model versions are listed in Table 1. Means and rms are weighted values calculated from the model residuals $e = d_{\text{obs}} - d_{\text{mod}}$ using the Huber weights w found in the last iteration.

The CHAOS-3 rms misfits for the satellite data are slightly lower than those of the CHAOS-2 model (cf. Table 1 of *Olsen et al.* [2009]). However, the observatory misfit is considerably lower (by a factor 2 for the horizontal components \dot{X} and \dot{Y} , and by about 30% for \dot{Z}) compared to CHAOS-2, probably due to the use of revised monthly mean values. In addition to the lower rms misfit, the non-zero means of the observatory \dot{X} and \dot{Z} that we found in CHAOS-2 are not present in CHAOS-3.

Figure 2 shows power spectra of the first time derivative (secular variation, circles) and of the second time derivative (secular acceleration, asterisks). CHAOS-3 has considerably higher secular acceleration power at degrees $n > 6$ compared to the two version of CHAOS-2s, which is due to the fact that the third time derivative of the field (and not the second time derivative) has been regularized. In addition, for CHAOS-3 the secular acceleration power are rather similar in 2005 and 2010.

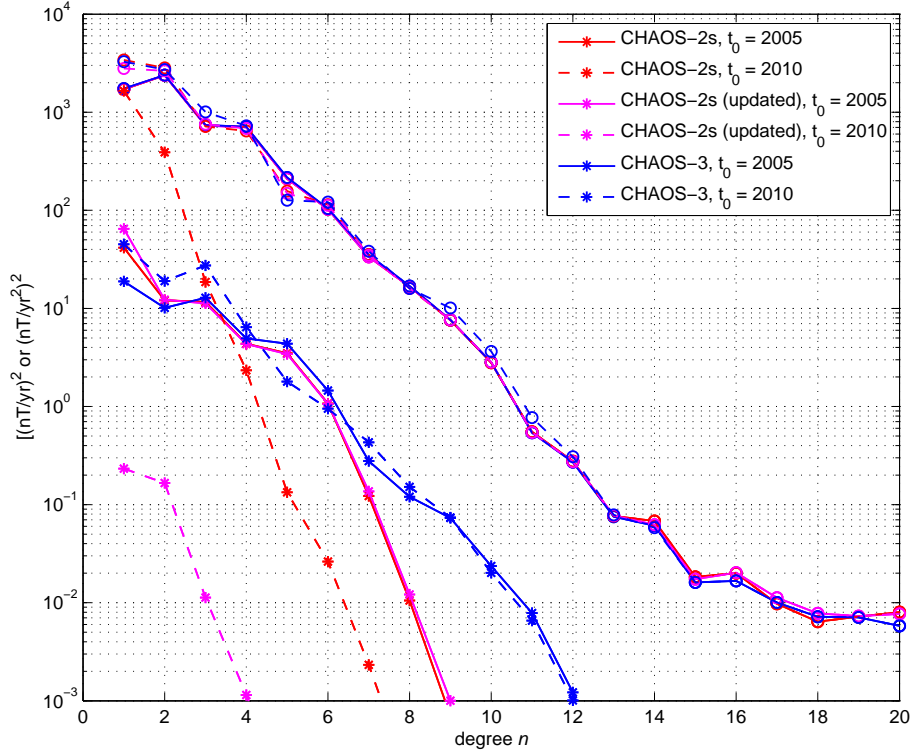


Figure 2: Power spectra of the first (circles) and second time derivative (asterisks) for epoch 2005 (solid lines), resp. 2010 (dashed lines) and the three models CHAOS-2s, “updated CHAOS-2s” and CHAOS-3.

Following the approach described in *Olsen and Manda* [2007] we calculated “virtual observatory” monthly means values for the January 2001 to August 2009, from which we derive time series of Gauss coefficients g_n^m and h_n^m . Figures 3 and 4, which are updates of Figs. 3 and 4 of *Olsen and Manda* [2007], show time series of the first time derivative, dg_n^m/dt and dh_n^m/dt , of the internal Gauss coefficients for $n = 1 - 6$. The symbols present annual differences of the coefficient, while the curves show model values from CHAOS-2s (red) and CHAOS-3 (blue). The magenta curve is for the “updated CHAOS-2s” model.

A comparison of the annual differences of (revised) observatory monthly means and model predictions are shown in Figures 5 and 6 for the 16 selected observatories shown with red symbols in Figure 1. These observatories are arranged according to their geographic latitude from North to South. The green symbols for the observatories KAK, HON, GNA and AMS represent revised hourly mean values that have been calculated after determination of CHAOS-3; these are thus independent data that have not been used in deriving the model.

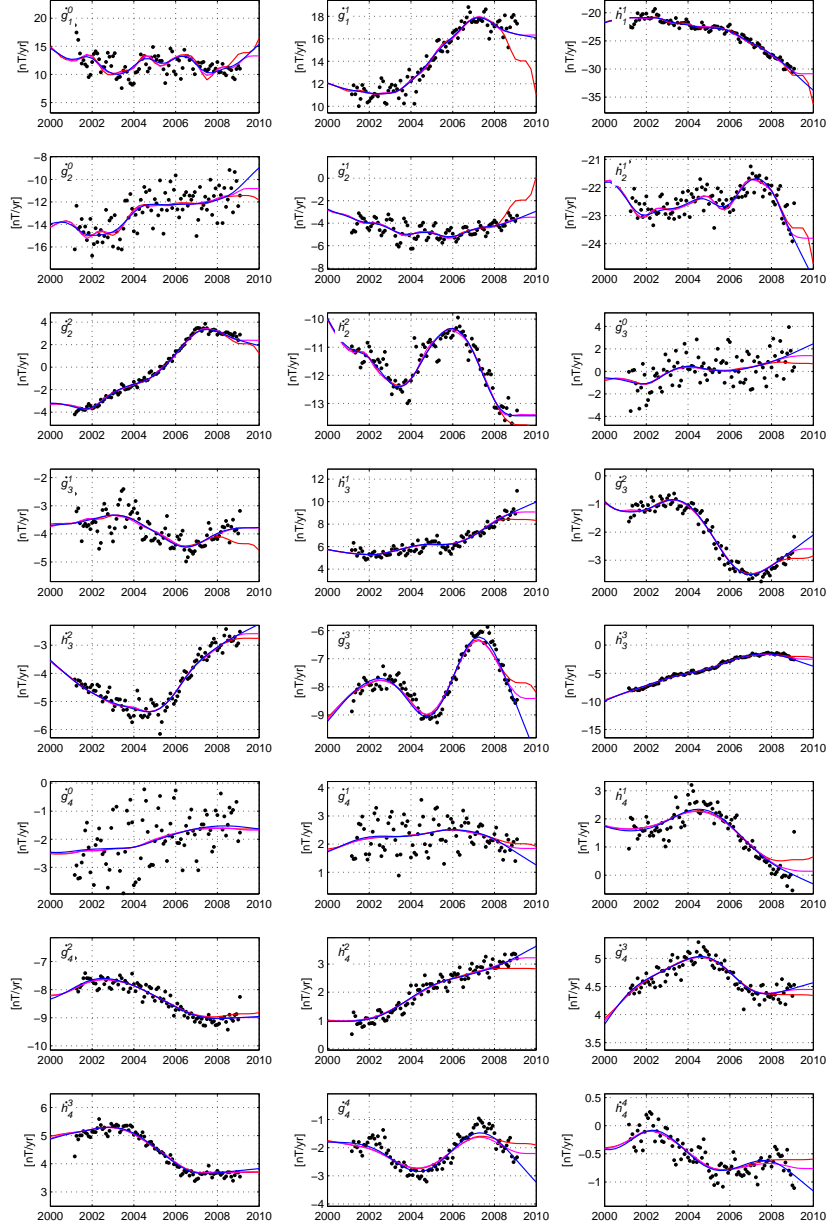


Figure 3: First time derivatives, dg_n^m/dt , dh_n^m/dt , of internal Gauss coefficients, in nT/yr. Symbols represent annual differences of time series of Gauss coefficients obtained from “virtual observatories” while the curves show and predictions of the *CHAOS-2s* (red), “*updated CHAOS-2s*” (magenta) and *CHAOS-3* (blue) models.

5 Extraction of the candidate models

From the parent model CHAOS-3 (internal name: CHAOS-3_09k_09) we have derived our three candidate models in the following way:

- **Candidate for DGRF-2005** is the degree $n = 1 - 13$ part of the parent model evaluated at epoch $t = 2005.0$. Filename is `DGRF-2005-DTU.dat`.
- **Candidate for IGRF-2010** is the degree $n = 1 - 13$ part of the parent model evaluated at epoch $t = 2010.0$. Note that 2010 is the last spline knot of the model, but since only data up to August 2009 have been used to determine the model this is an extrapolation in time beyond the data span. Filename is `IGRF-2010-DTU.dat`.
- **Candidate for average secular variation for 2010.0 to 2015.0** is the degree $n = 1 - 8$ part of the first time derivative of the parent model evaluated at epoch $t = 2010.0$. Filename is `IGRF-SV-2010-DTU.dat`.

Due to the difficulty to give sound error estimates for complicated models like CHAOS-3 we do not provide any number for the uncertainty of our candidate models (the corresponding columns in the files are set to zero).

In addition to these three candidate models we also provide the following test models for the average secular variation for 2010.0 to 2015.0:

- a degree 13 truncation of the secular variation for epoch 2010.0 as given by CHAOS-3. Filename is `IGRF-SV-extended-2010-DTU.dat`. Note that coefficients of degrees $n = 1 - 8$ of that model are identical to those of our candidate model `IGRF-SV-2010-DTU.dat`.
- a degree 13 truncation of the secular variation for epoch 2012.5 as given by the first and second time derivative of CHAOS-3 evaluated at $t_0 = 2010.0$: $\dot{g}_n^m|_{2012.5} = \dot{g}_n^m|_{2010.0} + (2012.5 - 2010.0) \cdot \ddot{g}_n^m|_{2012.5}$ (and similar for \dot{h}_n^m). Filename is `IGRF-SV-extended-2012-5-DTU.dat`. Note that this involves a quadratic extrapolation in time, which is expected to be very risky.

6 References

Maus, S., and P. Weidelt, Separating the magnetospheric disturbance magnetic field into external and transient internal contributions using a 1D conductivity model of the Earth, *Geophys. Res. Lett.*, *31*, L12,614, doi:10.1029/2004GL020,232, 2004.

Olsen, N., External field contributions in observatory monthly means, *Geophys. Res. Abstracts*, *11*, 2009.

Olsen, N., and M. Mandea, Investigation of a secular variation impulse using satellite data: The 2003 geomagnetic jerk, *Earth Planet. Science Lett.*, *255*, 94–105, doi:10.1016/j.epsl.2006.12.008, 2007.

Olsen, N., T. J. Sabaka, and F. Lowes, New parameterization of external and induced fields in geomagnetic field modeling, and a candidate model for IGRF 2005, *Earth, Planets and Space*, 57, 1141–1149, 2005.

Olsen, N., M. Manda, T. J. Sabaka, and L. Tøffner-Clausen, CHAOS-2 – A Geomagnetic Field Model Derived from one Decade of Continuous Satellite Data, *Geophys. J. Int.*, *in press*, 2009.

Sabaka, T. J., N. Olsen, and M. E. Purucker, Extending comprehensive models of the Earth's magnetic field with Ørsted and CHAMP data, *Geophys. J. Int.*, 159, 521–547, doi: 10.1111/j.1365-246X.2004.02421.x, 2004.

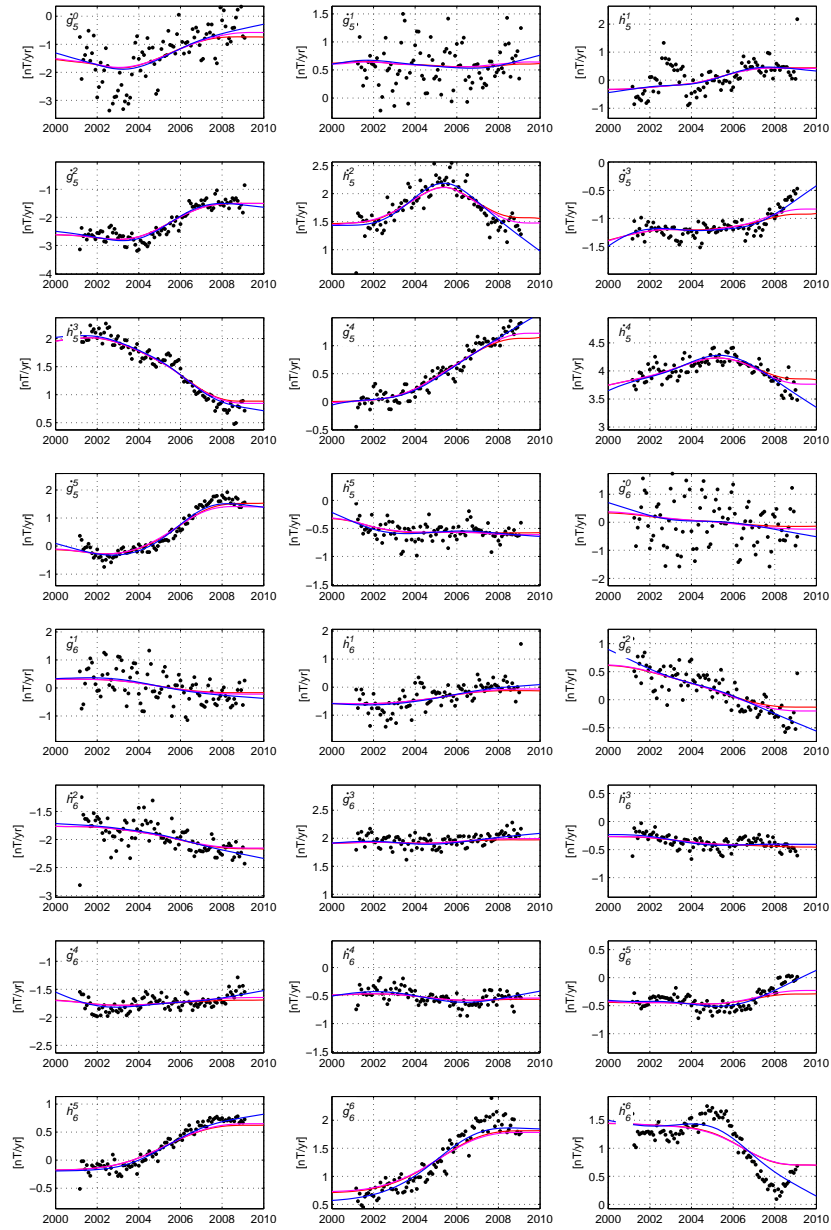


Figure 4: Continuation of Figure 3.

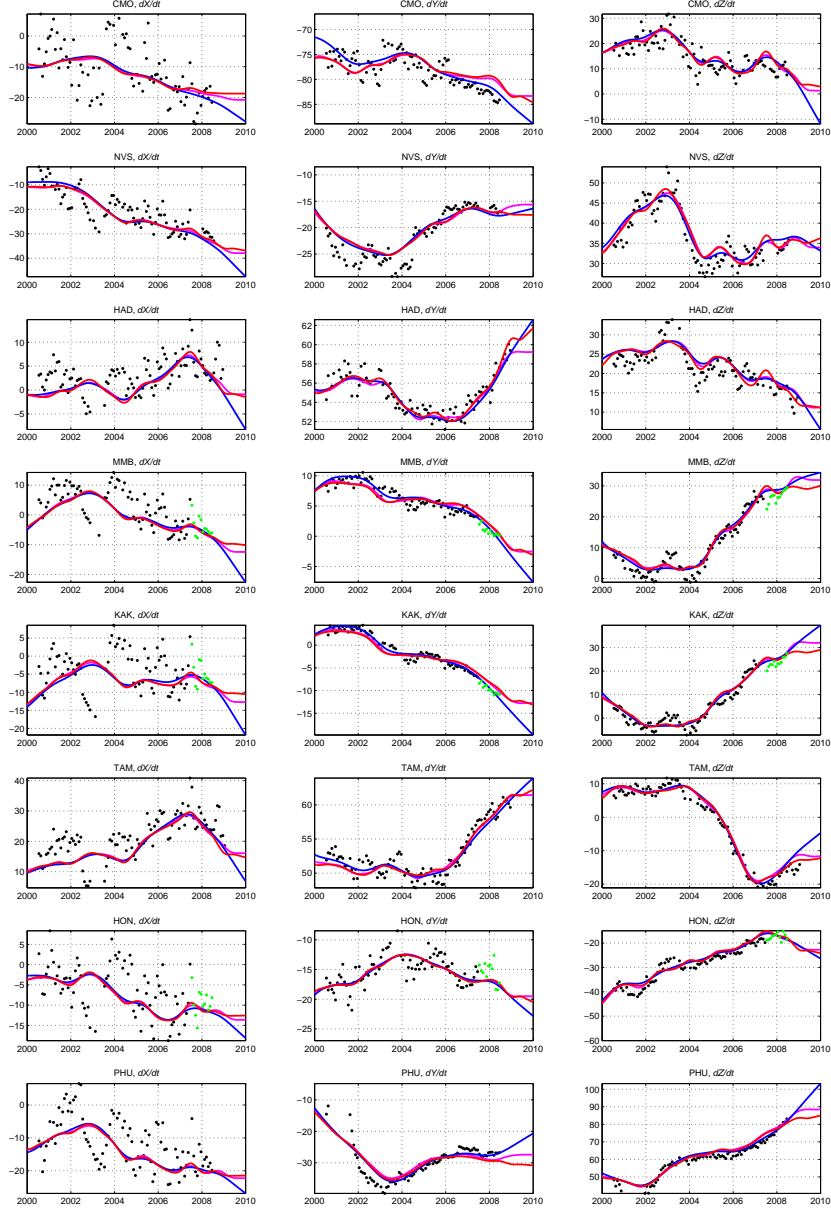


Figure 5: First time derivative of the vector components, dX/dt , dY/dt and dZ/dt at selected observatories. Symbols refer to observations (annual difference of revised monthly means), whereas the solid curves indicate predictions of the *CHAOS-2s* (red), “*updated CHAOS-2s*” (magenta) and *CHAOS-3* (blue) models.

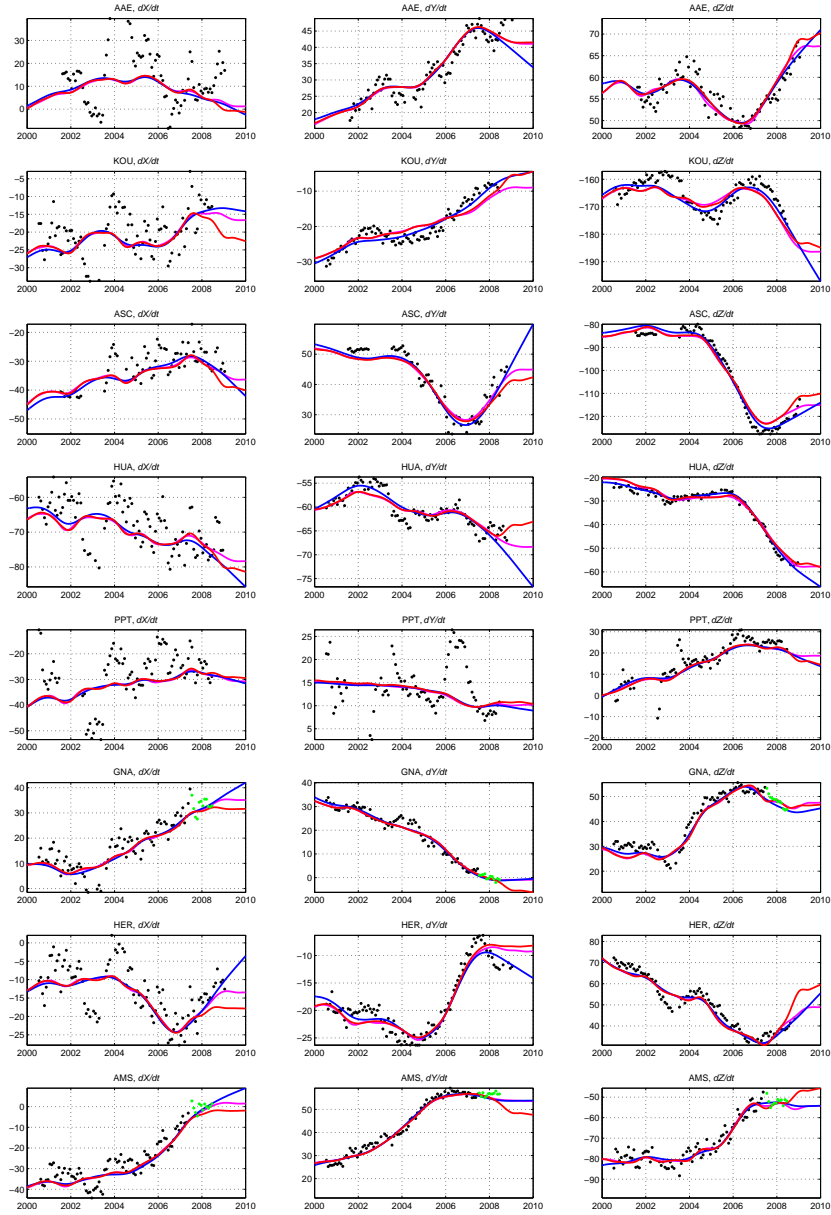


Figure 6: Continuation of Figure 5.